Conformations of the Noncovalent and Covalent Complexes between Mitomycins A and C and d(GCGCGCGC)$_2$

Shashidhar N. Rao, U. Chandra Singh, and Peter A. Kollman*

Contribution from the Department of Pharmaceutical Chemistry, University of California, San Francisco, California 94143. *Received January 22, 1985*

Abstract: We present molecular mechanics simulation of the noncovalent, monolinked covalent, and cross-linked covalent interactions of the potent and clinically useful anticancer agent mitomycin C with DNA. Major-groove binding appears to be favored over minor-groove binding, and there are low-energy noncovalent complexes with the reduced drug that orient their C1 and C10 atoms suitably to form covalent linkages with the O6 (N2) atoms of guanines in the major (minor) groove of the polynucleotide. Most of the complexes are characterized by an extensive network of hydrogen bonds between the drug and the polynucleotide. The molecular mechanical models predict stronger binding affinities for mitomycin C than for mitomycin A. The conformational features of the models provide initial focus for X-ray crystallographic analyses and physicochemical studies on the complexes between oligonucleotides and mitomycin.

Mitomycin C is known to be a potent and clinically useful antitumor agent and antibiotic that covalently attaches to the individual strands and forms cross-links between complementary strands of the DNA, leading to bacteriocidal and cytocidal effects.[1-13] These devastating effects are achieved despite the fact that DNA cross-links are found to occur at a frequency of 1 in 1000.[11,14] Monolinks by this drug are known to be 10-20 times more frequent than cross-links.[5,6] The drug requires metabolic activation to its effective form by a reductase system.[2]

Several investigators have concentrated their attention on understanding the chemical nature and the groups involved in the mitomycin binding to DNA. It was hypothesized that the C1 and C10 carbon atoms constituted the two reactive sites involved in the bifunctional cross-linking activity[11] and that C7 as a third reactive site could not be excluded.[15] Replacement of the amino group at C7 by the methoxy or the hydroxyl group was indicated not to greatly affect the lethal cross-linking activities of mitomycins.[11] In recent years, several bioreductive alkylation mechanisms have suggested C1 and C10 to be the binding sites during its active association with DNA[3,4,16] or RNA.[17] Subsequently, C1 has been confirmed to be one of the linking sites.[18]

Model building studies[19,20] on DNA-mitomycin complexes had postulated O6 and N7 atoms of guanines to be the possible alkylation sites, but the latter site was ruled out by tritium assay of mitomycin C-DNA reaction.[21] Recent solution studies on the modification of DNA with reductively activated mitomycin C point out that, in addition to O6, the drug can also covalently link to N2 of guanine residues to a much smaller extent than it can link to O6.[18,22] Tomasz and co-workers[23] have recently elucidated the full structure of a mitomycin C-dinucleoside monophosphate adduct using differential FT-IR spectroscopy, confirming O6 on guanine to be the linking site for the drug. They have also suggested N2 to be an important site of attack in the drug-RNA cross-linking reaction. In addition to the covalent linkages, mitomycin is also known to be capable of nonspecific binding to polynucleotides.[24,25]

Mitomycin-DNA complexes have been characterized by melting temperature,[26] circular dichroism,[27,28] transient electric dichroism,[29] and NMR studies.[28] Circular dichroism[27,28] studies indicated that the characteristic progressive changes observed in the MC-DNA complex was observed to a much greater extent in poly(dG-dC)·poly(dG-dC) than with either poly(dG)·poly(dC) or MC-RNA complexes. Transient electric dichroism studies of DNA and the synthetic polynucleotides in water/alcohol mixtures[29] and hydrodynamic studies[30] suggested that mitomycin was a strong factor in inducing Z DNA conformation in polynucleotides rich in G and C. However, recent ^{31}P NMR and radioimmunoassay studies[28] have ruled out Z DNA conformation in the mitomycin C-polynucleotide complexes and have interpreted the CD spectrum of MC-DNA complex in terms of an induced left-handed non Z conformation. However, the possibility of a drug-base interaction influencing the CD spectrum of B DNA has not been excluded.[28]

An important aspect of the structural studies on the mitomycin-DNA complexes is the configuration at C9, C9a, C1, and C2. Until recently, all the studies involving these complexes had indicated the configuration to be as predicted by the crystal structure determination of mitomycins A and B.[31,32] However, the absolute

(1) Matsumoto, I.; Lark, K. G. *Exp. Cell Res.* **1963**, *32*, 192-196.
(2) Lyer, V. N.; Szybalski, W. *Science (Washington, D.C.)* **1964**, *145*, 55-58.
(3) Moore, H. W. Science (*Washington, D.C.*) **1977**, *197*, 527-532.
(4) Franck, R. W. *Prog. Chem. Org. Nat. Prod.* **1979**, *37*, 1-45.
(5) Szybalski, W.; Lyer, V. N. *Microb. Genet. Bull.* **1964**, *21*, 16-17.
(6) Weissbach, A.; Lisio, A. *Biochemistry* **1965**, *4*, 196-200.
(7) Weiss, M. J.; Reding, G. S.; Allen, G. R., Jr.; Dornbush, A. C.; Lindsay, H. L.; Poleto, J. F.; Remers, W. A.; Roth, R. H.; Slobada, A. E. *J. Med. Chem.* **1968**, *11*, 742-745.
(8) Mercado, C. M.; Tomasz, M. *Antimicrob. Agents Chemother.* **1972**, *1*, 73-77.
(9) Small, G.; Setlow, J. I.; Kovistra, J.; Shapanka, R. J. *J. Bacteriol.* **1976**, *125*, 643-654.
(10) Balassa, G. *Ann. Inst. Pasteur, Paris* **1962**, *102*, 547-555.
(11) Szybalski, W.; Lyer, V. N. *Antibiotics (N.Y.)* **1967**, *1*, 211-245.
(12) Lyer, V. N.; Szybalski, W. *Proc. Natl. Acad. Sci. U.S.A.* **1963**, *50*, 355-362.
(13) Sekiguchi, M.; Takagi, Y. *Nature (London)* **1959**, *183*, 1134-1135.
(14) Sina, J. F.; Bean, C. L.; Dysart, G. R.; Taylor, V. I.; Bradley, M. O. *Mutat. Res.* **1983**, *113*, 357-391.
(15) Rao, K. V.; Biemann, K.; Woodward, R. B. *J. Am. Chem. Soc.* **1963**, *85*, 2532-2533.
(16) Kohn, H.; Zein, N. *J. Am. Chem. Soc.* **1983**, *105*, 4105-4106.
(17) Weaver, J.; Tomasz, M. *Biochim. Biophys. Acta* **1982**, *697*, 252-254.
(18) Hashimoto, Y.; Shudo, K.; Okamoto, T. *Chem. Pharm. Bull.* **1983**, *31*, 861-869.
(19) Szybalski, W.; Lyer, V. N. *Fed. Proc., Fed. Am. Soc. Exp. Biol.* **1964**, *23*, 946-949.
(20) Lipsett, M. N.; Weissbach, A. *Biochemistry* **1965**, *4*, 206-211.
(21) Tomasz, M. *Biochim. Biophys. Acta* **1970**, *213*, 288-295.
(22) Hashimoto, Y.; Shudo, K.; Okamoto, T. *Tetrahedron Lett.* **1982**, *23*, 677-680.
(23) Tomasz, M.; Lipman, R.; Snyder, J. K.; Nakanishi, K. *J. Am. Chem. Soc.* **1983**, *105*, 2059-2063.
(24) Lipman, R.; Weaver, J.; Tomasz, M. *Biochim. Biophys. Acta* **1978**, *521*, 779-791.
(25) Tomasz, M.; Lipman, R. *J. Am. Chem. Soc.* **1979**, *101*, 6063-6067.
(26) Cohen, R. J.; Crothers, D. M. *Biochemistry* **1970**, *9*, 2533-2539.
(27) Mercado, C. M.; Tomasz, M. *Biochemistry* **1977**, *16*, 2040-2046.
(28) Tomasz, M.; Barton, J. K.; Magliozzo, C.; Tucker, D.; Lafer, E. M.; Stollas, B. D. *Proc. Natl. Acad. Sci. U.S.A.* **1983**, *80*, 2874-2878.
(29) Wu, H. M.; Dattagupta, N.; Crothers, D. M. *Proc. Natl. Acad. Sci. U.S.A.* **1981**, *78*, 6808-6811.
(30) Kaplan, D. J.; Tomasz, M. *Biochemistry* **1982**, *21*, 3006-3103.
(31) Tulinsky, A.; van den Hende, J. H. *J. Am. Chem. Soc.* **1967**, *89*, 2905-2911.
(32) Yahashi, R.; Matsubara, I. *J. Antibiot.* **1976**, *29*, 104-106.

0002-7863/86/1508-2058$01.50/0

configuration of this drug has been revised on the basis of crystallographic analysis of 1-*N*-(*p*-bromobenzoyl)mitomycin C.[33] In our investigations, we have used the latter configuration.

Relative activity of various derivatives of mitomycin has been an area of intense research in recent years. It was earlier suggested that mitomycin A was a better cross-linker than mitomycin C and that it had similar or sometimes slightly lower antitumor activity than the latter.[11] An adaptive least-squares classification applied to structure–activity correlation of antitumor mitomycin derivatives reveals that mitomycin C displays stronger activity than mitomycin A,[34] as implied by earlier studies.[35] Mitomycin A is believed to be more potent than mitomycin C but less effective than the latter[36] (Remers, W.; Bradner, W., personal communication).

A number of theoretical analyses of drug–DNA interactions have been reported.[37-44] Most of these investigations have dealt with sequence selectivity in short base-paired nucleic acid fragments (two to four nucleotides long) for intercalation of drugs such as ethidium, daunomycin, and proflavin. Monocovalent complexes with tri- and tetranucleotides have also been investigated for a few drugs and carcinogens.[43,44] To our knowledge, the study presented here is the first in which noncovalent (intercalation and nonintercalation), monolinked, and cross-linked covalent interactions of a drug and DNA have been analyzed with the state-of-the-art computer graphics and molecular mechanics in which all degrees of freedom have been energy refined. Although the models suffer from the inaccuracies of the potential functions and limited search of local minima on the potential surface, they provide an initial focus for experimental work (2D NMR/NOE measurements or crystallographic studies) that may allow them to be further refined.

In this study, we have carried out model building and energy-refinement studies on complexes of DNA with mitomycins C and A to suggest high-resolution models for these structures. Consistent with experiments (vide infra), we find that the binding probability of mitomycin C to polynucleotides is higher in the major groove than in the minor groove. We have found low-energy noncovalent structures that place the drug in the major and the minor grooves and, respectively, the O6 and N2 (in guanines) in excellent positions to attack the aziridinium ring and form the monolinked structures. Further, in the monolinked complexes, the acetylamide group of the mitomycin is in a perfect position for covalent attack on the guanine O6 and N2 atoms on the neighboring G–C base pair in, respectively, major-groove and minor-groove binding, and such an attack can lead to cross-linked structures.

Methods

We have modeled the interaction of a DNA duplex with mitomycin A and mitomycin C (referred to henceforth as MA and MC, respectively) by considering the decanucleotide d(GCGCGCGCGC)$_2$ (referred to henceforth as GC10) in the B form. It may be noted that this sequence represents one full turn of the B DNA helix. We emphasize that, in view of the lack of Z DNA conformation in DNA–mitomycin complexes as evidenced by experimental studies summarized in the previous section, we did not attempt model building with a Z DNA decamer. In order to understand the long-range effects of the complexation, we have "bound" the drugs in the central portion of the sequence, as has been described below.

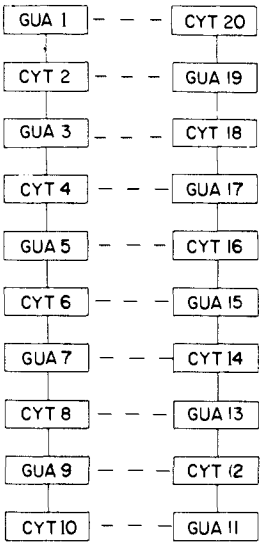

Figure 1. Schematic illustration of nomenclature used in describing the decanucleotide d(GCGCGCGCGC)$_2$ (referred to as GC10 in the text).

The conformational analyses in the present investigations were carried out by using the methods of molecular mechanics, wherein energy calculations were performed with the program AMBER (assisted model building with energy refinement).[45] We have employed the force field parameters presented by Weiner et al.[46] The molecular mechanical energies were evaluated by using eq 1 and the structures were refined

$$E_{\text{total}} = \sum_{\text{bonds}} K_r(r - r_{\text{eq}})^2 + \sum_{\text{angles}} K\vartheta(\vartheta - \vartheta_{\text{eq}})^2 + \sum_{\text{dihedrals}} \frac{V_n}{2}[1 + \cos(n\phi - \gamma)] + \sum_{i<j}\left[\frac{A_{ij}}{R_{ij}^{12}} - \frac{B_{ij}}{R_{ij}^{6}} + \frac{q_i q_j}{\epsilon R_{ij}}\right] + \sum_{\text{H-bonds}}\left[\frac{C_{ij}}{R_{ij}^{12}} - \frac{D_{ij}}{R_{ij}^{10}}\right] \quad (1)$$

until the root-mean-square gradient was less than 0.1 kcal/mol Å. In all the calculations, we have used a distance-dependent dielectric constant $\epsilon = R_{ij}$. The charges on MC and MA were obtained by using quantum chemically derived electrostatic potentials[47] and are described in Appendix I.

We have supplemented the force field parameters[46] with appropriate bond length, bond angle, and dihedral parameters corresponding to the additional atom types defined in MA and MC. Also, we have defined new atom types for some of the atoms of the guanine bases that are involved in covalent linkages with the drugs and have supplemented the corresponding force field parameters. These are described in Appendix II.

For the sake of convenience, the following nomenclature has been used in designating residues of GC10. Residues have been counted from the 5′ end to the 3′ end of each strand as GUA1, CYT2, GUA3, CYT4, etc. Thus, the last residue at the 3′ end of the second strand would be referred to as CYT20. Figure 1 schematically illustrates this nomenclature. Also, the phosphate groups have been referred to as P_{n-m}, where n and m are the serial numbers of the bases at, respectively, the 5′ and 3′ ends. For example, the phosphate group intervening GUA3 and CYT4 is designated as P_{3-4}.

Figure 2a shows the protonated 7-aminomitosene moiety, which has been used in the study of noncovalent complexes with GC10. This moiety is likely to be a stable intermediate structure in the pathway of reduction of mitomycin C to its biologically active form. Compounds closely related to this intermediate have been isolated and characterized by UV and IR spectroscopy.[48] Parts b and c of Figure 2 show schematic representations of MC in its biologically active form when covalently monolinked and cross-linked to the polynucleotide, respectively. Dashed lines in these

(33) Shirahata, K.; Hirayama, N. *J. Am. Chem. Soc.* **1983**, *105*, 7199–7200.
(34) Moriguchi, I.; Komatsu, K. *Chem. Pharm. Bull.* **1977**, *25*, 2800–2802.
(35) Kinoshita, S.; Uzu, K.; Nakano, K.; Shimizu, M.; Takahashi, T. *J. Med. Chem.* **1971**, *14*, 103–109.
(36) Iyengar, B. S.; Lin, H.-J.; Cheng, L.; Remers, W. A. *J. Med. Chem.* **1981**, *24*, 975–981.
(37) Pack, G. R.; Loew, G. H. *Biochim. Biophys. Acta* **1978**, *519*, 163–172.
(38) Ornstein, R. L.; Rein, R. *Biopolymers* **1979**, *18*, 2821–2847.
(39) Nuss, M. E.; Marsh, F. J.; Kollman, P. A. *J. Am. Chem. Soc.* **1979**, *101*, 825–833.
(40) Miller, K. J.; Brodzinsky, R.; Hall, S. *Biopolymers* **1980**, *19*, 2091–2122.
(41) Nakata, Y.; Hopfinger, A. J. *Biochem. Biophys. Res. Commun.* **1980**, *95*, 583–588.
(42) Aggarwal, A. K.; Islam, S. A.; Neidle, S. *J. Biomol. Struct. Dyn.* **1983**, *1*, 873–881.
(43) Taylor, E. R.; Miller, K. J.; Bleyer, A. J. *J. Biomol. Struct. Dyn.* **1983**, *1*, 883–904.
(44) Lybrand, T. P.; Kollman, P. A. *Biopolymers*, in press.
(45) Weiner, P. K.; Kollman, P. A. *J. Comput. Chem.* **1981**, *2*, 287–303.
(46) Weiner, S. J.; Kollman, P. A.; Case, D.; Singh, U. C.; Ghio, C.; Alagona, G.; Profeta, S., Jr.; Weiner, P. K. *J. Am. Chem. Soc.* **1984**, *106*, 765–784.
(47) Singh, U. C.; Kollman, P. A. *J. Comput. Chem.* **1984**, *5*, 129–145.
(48) Patrick, J. B.; Williams, R. P.; Meyer, W. E.; Fulmor, W.; Cosulich, D. B.; Broschard, R. W.; Webb, J. S. *J. Am. Chem. Soc.* **1964**, *86*, 1889–1890.

Table I. Hydrogen Bond Parameters (Involving the Drug–Polynucleotide Interactions) in the Noncovalent and Covalent Complexes between Mitomycin C and Mitomycin A and $d(GCGCGCGCGC)_2$[a]

complex	X	Z	length: H--Z	angle: X–H–Z
NC_1	N10A (MIT)	OA (P_{13-14})	1.69	150.0
	N7 (MIT)	OA (P_{14-15})	1.69	158.9
	N2 (MIT)	OA (P_{3-4})	1.65	142.7
	N4 (CYT14)	O10A (MIT)	1.97	156.4
NC_2	N2 (MIT)	O2 (CYT6)	1.73	144.2
	N2 (GUA17)	O10A (MIT)	1.84	157.0
NCl_1	N2 (MIT)	OA (P_{4-5})	1.64	142.8
	N10A (MIT)	O2 (CYT6)	1.87	147.9
	N2 (MIT)	O6 (GUA15)	1.74	157.8
NCl_2	N10A (MIT)	OA (P_{15-16})	1.65	163.9
	N2 (MIT)	O2 (CYT6)	1.69	158.4
M_{a1}	N10A (MIT)	OA (P_{13-14})	1.68	151.9
	N7 (MIT)	OA (P_{14-15})	1.70	152.5
	N2 (MIT)	OA (P_{3-4})	1.62	160.3
	N4 (CYT14)	O10A (MIT)	1.92	153.1
M_{a2}	N7 (MIT)	OB (P_{17-18})	1.75	141.4
	N2 (MIT)	O2 (CYT6)	1.76	142.2
	N2 (GUA17)	O10A (MIT)	1.90	158.0
M_{N7}	N10A (MIT)	OA (P_{13-14})	1.69	151.7
	N7 (MIT)	OA (P_{14-15})	1.67	159.1
	N2 (MIT)	OA (P_{3-4})	1.62	169.5
	N2 (MIT)	OA (P_{4-5})	1.65	148.6
	N4 (CYT14)	O10A (MIT)	1.92	152.4
M_h	N10A (MIT)	OA (P_{13-14})	1.66	156.0
	N7 (MIT)	OA (P_{14-15})	1.70	147.6
	N2 (MIT)	OA (P_{3-4})	1.65	138.3
	N4 (CYT14)	O10A (MIT)	1.89	146.4
MA_{m1}	N10A (MIT)	OA (P_{13-14})	1.68	152.8
	N2 (MIT)	OA (P_{3-4})	1.62	165.4
	N4 (CYT14)	O10A (MIT)	1.92	153.2
MA_{c1}	N2 (MIT)	OA (P_{3-4})	1.62	175.5
C_1	N7 (MITe	OA (P_{14-15})	1.72	147.0
	N2 (MIT)	OA (P_{3-4})	1.62	166.2
C_2	N7 (MIT)	OA (P_{4-5})	1.73	143.3
	N2 (MIT)	O6 (GUA7)	1.71	165.5
C_3	N7 (MIT)	OB (P_{17-18})	1.76	146.3
	N2 (MIT)	O2 (CYT6)	1.78	140.2
MA_{m2}	N2 (MIT)	O2 (CYT6)	1.74	144.9
	N2 (GUA17)	O10A (MIT)	1.90	156.3
MA_{c2}	N2 (MIT)	O2 (CYT6)	1.75	146.6

[a] In a hydrogen bond X--H···Z, X and Z are, respectively, donor and acceptor atoms, with H being the hydrogen atom. The hydrogen bond lengths and angles are in angstroms and degrees, respectively.

figures indicate the points of covalent linkages. Thus, in monolinked complexes, C1 is linked to O6 (major-groove binding) or N2 (minor-groove binding) of guanine, while in the cross-linked complexes, in addition, C10 is also covalently attached to these atoms.

It may be noted that, in both MA and MC, the amino group attached at C2 has a p*K* value of around 8. Hence, at physiological pH this group will be protonated, and in the present investigations, in both monolinked and cross-linked complexes between these drugs and DNA, we have retained a protonated amino group attached to C2 (parts b and c of Figure 2). Also, consistent with the revised absolute configuration,[33] this group is in an axial orientation relative to the five-membered ring formed by the atoms C1, C2, C3, N4, and C9a. We have studied the following cases of the mitomycin–DNA complexes in the present investigations. In all of them the starting geometry of GC10 was a standard B DNA one.[49]

Results

In most of the DNA–mitomycin complexes investigated in the present study, the polynucleotide backbone and glycosidic conformations are very similar to those found in a B DNA structure. The latter has gauche$^+$, trans, trans, gauche$^-$, gauche$^-$, and anti conformations about the C4′–C5′, C3′–O3′, C5′–O5′, P–O3′, P–O5′, and glycosidic bonds with C2′ endo sugars. Therefore, our discussions on the conformational aspects of the polynucleotide part in the complexes have been restricted to only those cases where the deviations are significant as compared to those in the standard B DNA. Also the energy refinement of GC10 yielded a structure whose conformational features were very close to those of the B DNA[49] and hence not discussed in this paper.

Table II. Total Energies and Drug, Drug–Helix, Helix, and Polynucleotide Destabilization Energies (in kcal/mol) of the Covalent and Noncovalent Complexes between Mitomycin and $d(GCGCGCGCGC)_2$

complex	total energy	drug energy	drug–helix energy[a]	helix energy[b]	helix destabilizn[c]
M_{a1}	−962.3	−0.5	−151.1	−810.7	39.7
M_{a2}	−970.5	0.2	−146.9	−824.1	26.3
C_1	−904.1	25.4	−146.3	−783.2	67.2
C_2	−903.3	26.3	−150.0	−779.6	70.8
C_3	−930.7	20.6	−148.8	−802.5	47.9
MA_{m1}	−954.3	−1.8	−141.3	−811.2	39.2
MA_{m2}	−964.7	3.2	−136.9	−824.6	25.8
MA_{c1}	−900.6	21.8	−137.9	−784.5	65.9
MA_{c2}	−928.3	19.2	−139.8	−807.7	42.7
NC_1	−984.7	−2.4	−149.3	−833.0	17.4
NC_2	−964.8	−8.6	−115.0	−841.2	9.2
NCl_1	−981.1	−7.2	−149.7	−824.2	26.2
NCl_2	−960.6	−6.6	−123.8	−830.2	20.2

[a] Drug–helix energy is the energy of interaction between the atoms of the drug and those of the polynucleotide. [b] Helix energy is the energy of the polynucleotide part of the drug–DNA complexes. [c] Helix destabilization energy is the difference in energies of refined CC10 (−850.4 kcal/mol) and the polynucleotide part of the complexes.

One of the most striking conformational features in the DNA–mitomycin complexes is their stabilization by hydrogen bonds between MC and the polynucleotide. Table I lits the parameters such as donor and acceptor atoms, lengths (distances between the hydrogens and the acceptors), and angles (formed at the hydrogen atoms) for these hydrogen bonds in all the complexes. For the sake of convenience of description of sugar puckers, we have divided the phase (W) space into three broad regions. In accordance with this classification, W values from 0 to 72, 72 to 144°, and 144 to 180° correspond to sugar puckers in the C3′ endo, O1′ endo–C1′ exo, and C2′ endo regions. In the case of intermediate sugar puckers (O1′ endo–C1′ exo) the phases of individual sugar moieties are explicitly mentioned.

Futher, we note that a comparison of total energies is only possible within a given class of structures (e.g. noncovalent, monolinked to N2, and monolinked to O6 are three different classes). In addition, the drug–helix interaction energy and the helix destabilization energy (also called the polynucleotide strain energy) can be qualitatively compared when comparing various classes of complexes. The latter is defined as the difference between the total energy of the refined structure of GC10 and that of the polynucleotide part of the drug–DNA complexes. These energy components together with the total energies of the complexes have been listed in Table II. To obtain a detailed understanding of such interactions, we have carried out component analysis of the total energies of these complexes wherever necessary. In these analyses, sugars, bases, and phosphates are treated as individual groups. The phosphate group includes both O3′ and O5′ atoms. In addition, the drug in each complex is treated as a separate group. The energies of interactions between various groups have been indicated by appropriate arrows connecting the groups.

(1) Noncovalent Complexes between GC10 and Mitomycin C. These complexes have been investigated in order to understand the mechanism of covalent complex formation. As mentioned earlier,[24] at high concentrations, reductively activated MC exhibits a strong, nonoovalont electrostatic binding to nuclcic acids. It is likely that the noncovalent complex may be in an appropriate conformation to lead in a facile manner to drug–DNA covalent binding. We constructed two preliminary models of this complex by using interactive computer graphics and the program CHEM[50]

(49) Arnott, S.; Campbell-Smith, P.; Chandrasekaran, R. in *CRC Handbook of Biochemistry*; Fasman, G. D., Ed.; CRC: Cleveland, OH **1976**; Vol. 2, pp 411–422.

(50) Dearing, A. CHEM Program Written at the UCSF Computer Graphics Laboratory, 1981.

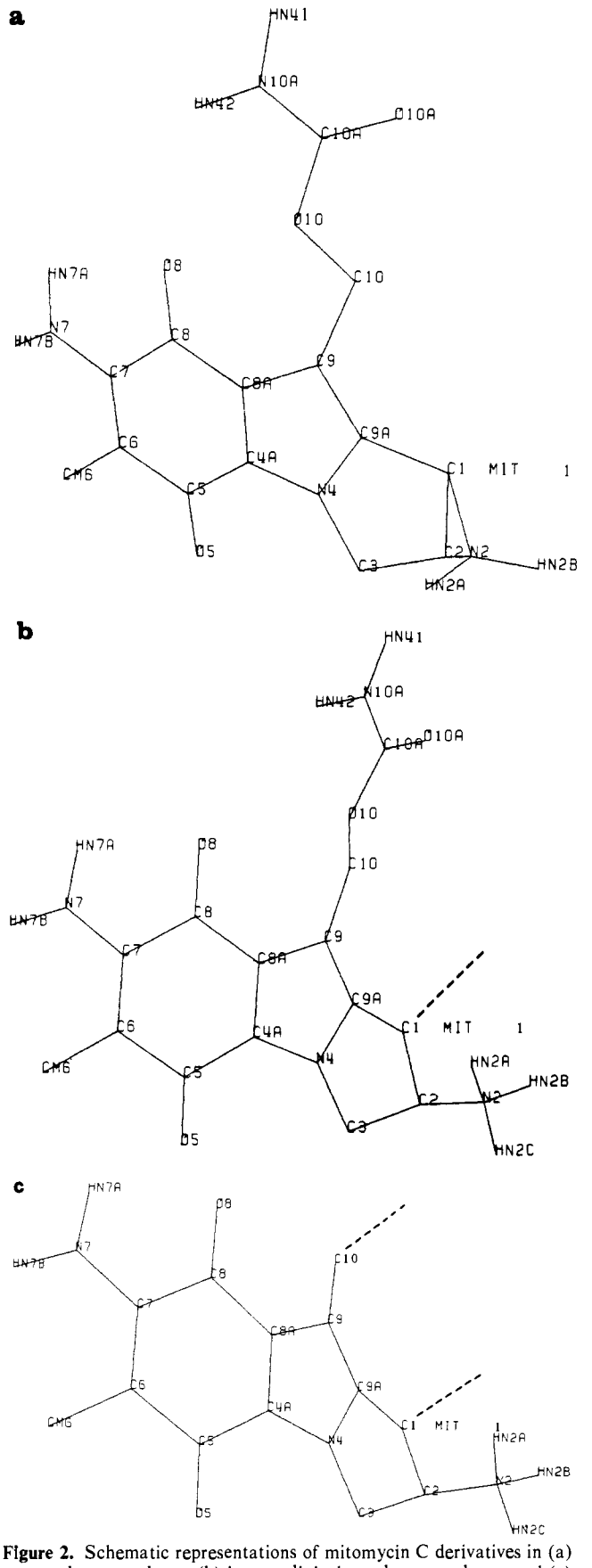

Figure 2. Schematic representations of mitomycin C derivatives in (a) noncovalent complexes, (b) in monolinked covalent complexes, and (c) cross-linked covalent complexes. The dashed lines in (b) and (c) indicate the points of covalent attachment on the drug.

by "docking" the 7-aminomitosene moiety shown in Figure 2a into the major and minor grooves of GC10 in the region around the base pair GUA5–CYT16. This was done with the covalent

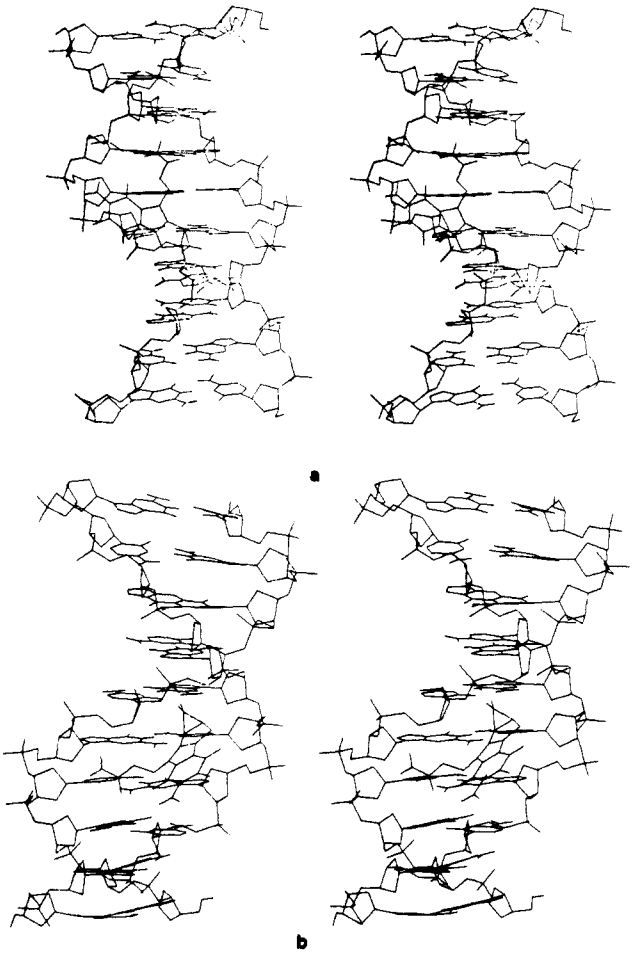

Figure 3. Stereopairs of the noncovalent nonintercalation complexes between GC10 and 7-aminomitosene with (a) the drug docked in the major groove and (b) the drug docked in the minor groove of the decanucleotide.

complexes between mitomycin C and GC10 in view. The energy-refined models are referred to as NC_1 and NC_2, corresponding to the drug in the major and minor grooves, respectively.

In both NC_1 and NC_2 (Figure 3, parts a and b, respectively), on the sugars in CYT2, CYT12, and GUA13 have O1′ endo–C1 exo pucker different from those of the normal C2′ endo sugars found in the rest of the structures. The phase angles corresponding to these sugars are, respectively, 114°, 119°, and 107° in NC_1 and 125°, 123°, and 119° in NC_2. Also in NC_1, the P–O3′ conformation at the 3′ ends of GUA3, GUA7, and GUA15 residues are trans instead of the gauche$^-$ found in NC_2 and the energy-refined GC10.

In NC_1, the acceptor atoms in the first three of the N--H···O hydrogen bonds are, respectively, one of the pendant oxygens on P_{3-4}, P_{13-14}, and P_{14-15}. The corresponding nitrogen atoms in MC are N2, N10A, and N7, respectively. The fourth hydrogen bond involves the NH_2 group on CYT14 and O10A in MC. The complex NC_2, on the other hand, is stabilized by only two hydrogen bonds (both N--H···O) between MC and the polynucleotide. One of them involves HN2B of GUA17 while the other involves O2 of CYT6. The corresponding atoms on the drug are, respectively, N2 and O10A. The stabilization of the polynucleotide by Watson–Crick hydrogen bonds is not significantly affected by the formation of these two noncovalent complexes.

We have also model built two intercalation complexes in which the 7-aminomitosene moiety in Figure 2a was "inserted" in between the base pairs GUA5–CYT16 and GUA15–CYT6 from the major- and minor-groove sides. Energy-refined models corresponding to these starting structures are termed as NCl_1 (Figure 4a) and NCl_2 (Figure 4b), respectively. They differ from the normal B DNA structure mainly around the site of intercalation. The C4′–C5′ torsion in CYT16 is trans instead of the gauche$^+$

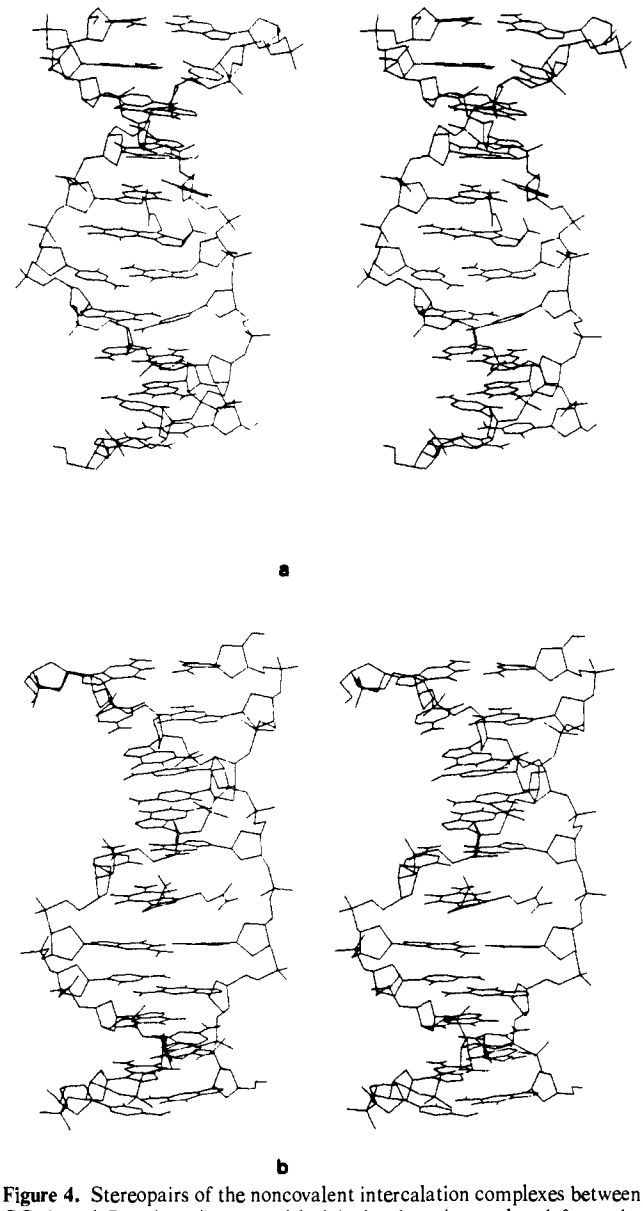

Figure 4. Stereopairs of the noncovalent intercalation complexes between GC10 and 7-aminomitosene with (a) the drug intercalated from the major-groove and (b) the drug intercalated from the minor-groove sides of the decanucleotide.

in the rest of the structures and CG10. This change is reflected in the phosphodiester conformations between GUA15 and CYT16, which are trans,trans instead of the gauche$^-$,gauche$^-$ in GC10. The trans conformations about P–O3′ occur at the 3′ ends of CYT4 and GUA15, and the sugars of GUA13 and GUA17 in NCl_1 and GUA13 and CYT2 in $NC2_2$ have O_1' endo–C1′ exo geometries. From Table I, we can see that these models are energetically slightly less favorable than those for the nonintercalation complexes. Our attempts to build an intercalation complex with mitomycin, having the more commonly observed gauche$^-$,gauche$^-$ phosphodiester conformations instead of trans,trans as in the above models, have yielded energetically less favorable structures than NCI_1 (in the major groove) and NCI_2 (in the minor groove).

In the intercalation complexes, in addition to stabilization by hydrogen bonds between MC and the polynucleotide, there is a destablization of the latter's helical structure due to reduced base pair–base pair interaction energy between CYT6–GUA15 and GUA5–CYT16. This feature is qualitatively consistent with that obtained from earlier investigations that had indicated that creation of an intercalation site is energetically costly.[39,51] However, recent investigations on daunomycin–DNA interactions[52] have suggested that the energy required for the creation of intercalation sites in a B DNA tetramer would be less than zero for certain sequences, particularly those with the pyrimidine–purine sequence constituting the central two base pairs. However, the corresponding energy value for the CGCG sequence (employed in the present investigations) is evaluated to be around 6.0 kcal/mol,[52] also qualitatively consistent with our findings. While there are three N--H···O hydrogen bonds in NCI_1 (involving O2 of CYT6, O6 of GUA15, and one of the pendant oxygens on P_{4-5}), only two of them stabilize NCI_2 (involving O2 of CYT6 and one of the pendant oxygens on P_{15-16}) (Table I).

(2) Monolinked Complexes between MC and GC10. Here, we have considered the major-groove and the minor-groove complexes between the polynucleotide and the drug. The energy-refined model is referred to as M_{a1} when the drug is in the major groove of the polynucleotide and as M_{a2} when the drug is in the minor groove. In the former, the covalent bond between the drug and the polynucleotide is formed between C1 of MC and O6 of GUA5, while in the latter, it is with N2 of GUA5.

Drug in the Major Groove. In M_{a1} (Figure 5a), as in the noncovalent complexes NC_1 and NC_2, the sugar puckers corresponding to CYT2 and CYT12 have O1′ endo–C1′ exo puckers ($W \sim 100°$). The P–O_3' conformation is trans at the 3′ ends of GUA3, GUA5, GUA7, CYT8, GUA13, and GUA15. As in NC_1, M_{a1} is stabilized by four hydrogen bonds between MC and the polynucleotide. The various groups involved in these hydrogen bonds are the same as in NC_1.

Drug in the Minor Groove. In M_{a2} (Figure 5b), the sugars in CYT2, GUA3, CYT12, GUA13, and CYT18 have geometries in the O1′ endo–C1′ exo region with phase angles of 131°, 104°, 136°, 137°, and 140°. the trans conformations about the P–O3′ bond occur at the 3′ ends of CYT6, CYT8, GUA15, and CYT18. M_{a2} is stabilized by three hydrogen bonds between MC and the polynucleotide. The acceptor atoms are, respectively, one of the pendant oxygens on P_{17-18}, O2 in CYT6, and O10a in MC. The corresponding donor nitrogen atoms are N7 and N1 on MC and N2 of GUA17.

An examination of the noncovalent complex NC_1 reveals that the C1 atom of mitomycin is also in a suitable environment to attack the N7 of GUA5. As mentioned earlier, several experimental studies have ruled out N7 alkylation by mitomycin C. We therefore sought to rationalize qualitatively such an observation through molecular mechanical calculations and model built and energy refined a corresponding monolinked complex (M_{N7}). This complex has a few interesting conformational features different from those of M_{a1}. First, unlike the latter, in M_{N7} (Figure 5c), all the base pairs, including the GUA5–CYT16 base pair, are intact as in GC10. This is not surprising since the covalently linked guanine in GUA5 is not "pulled" into the major groove as in M_{a1}. Second, the complex is stabilized by five hydrogen bonds between mitomycin C and the decamer (Table I). However, the distance between N7 atoms on guanines involved in neighboring base pairs is of the order of 7 Å and is too large for the cross-linked complex without drastic conformational alterations in the polynucleotide structure.

We have also model built and energy refined a complex between MC and poly(dG)·poly(dC) with a view to examine the sequence specificity of mitomycin binding. It is obvious that, in such a complex (M_h; Figure 5d), cross-links involving O6 atoms of guanine bases are out of question as they are on the same strand. Also, in such structures, the possibility of neighboring guanines being linked through mitomycins exists only at the expense of large distortions in the polynucleotide structure. However, monolinked complexes are possible in this case, with the stabilization between the drug and the polynucleotide being achieved through a set of hydrogen bonds very similar to those in M_{a1} (Table I).

Energetics of Monolinked Complexes. Figure 6 shows the component analysis diagrams corresponding to M_{a1} and M_{a2}. In

(51) Ornstein, R. L.; Rein, R. *Biopolymers* **1979**, *18*, 1877–1890.

(52) Newlin, D. D.; Miller, K. J.; Pilch, D. F. *Biopolymers* **1984**, *23*, 139–158.

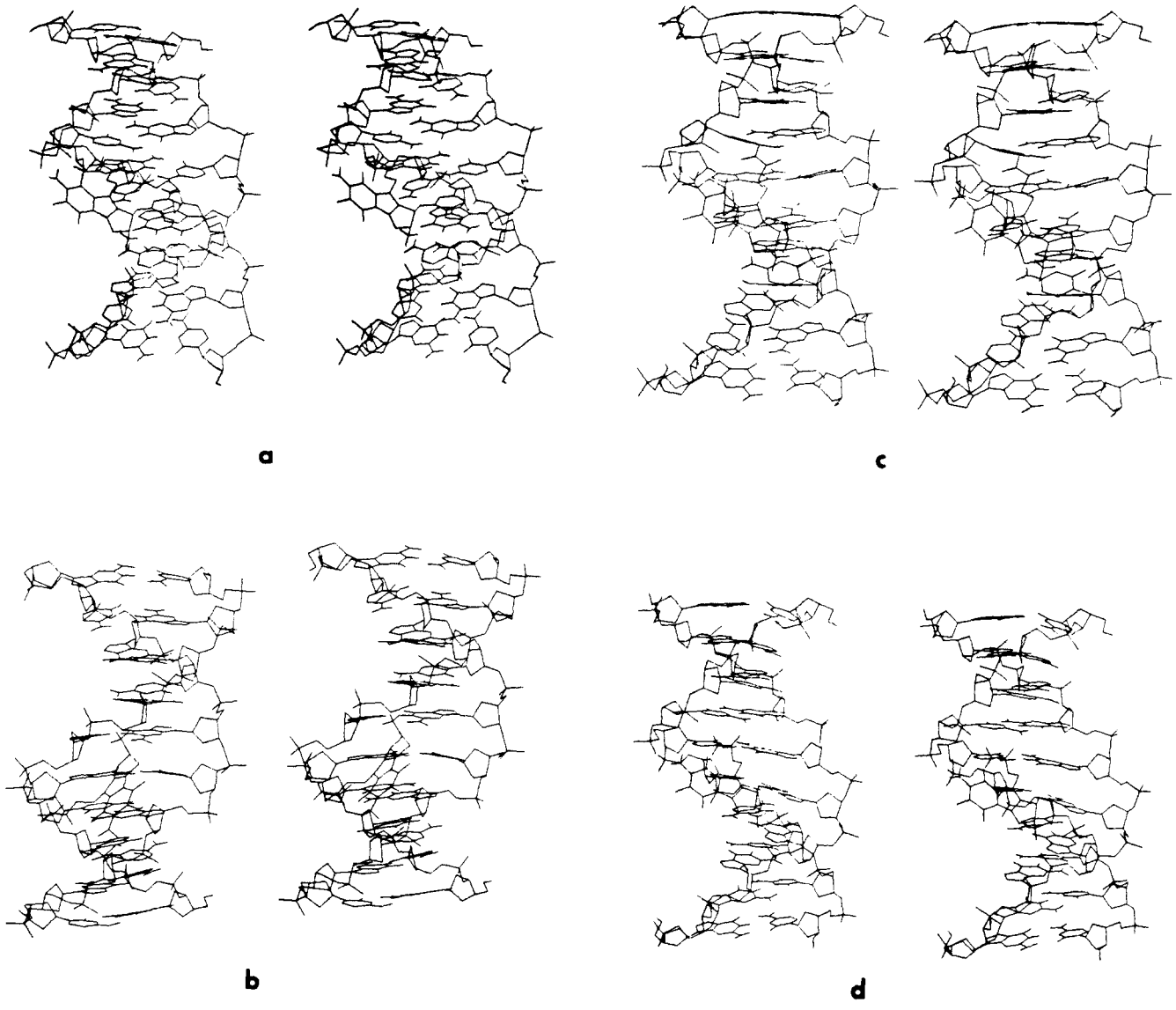

Figure 5. Stereopairs of the monolinked covalent complexes between MC and GC10 with (a) the drug in the major groove (O6 attack), (b) the drug in the minor groove (N2 attack), and (c) the drug in the major groove (N7 attack). The stereopair of a covalent complex between MC and poly(dG)·poly(dC) involving O6 of guanine is illustrated in (d).

both these diagrams, the stabilization of the two complexes by networks of hydrogen-bonding interactions is evident through the total energy terms between the drug and various groups on the polynucleotide. The polynucleotide strain energy is higher in the major-groove complex than in the minor-groove complex. In the former, the polynucleotide strain arises mainly due to the disruption of the hydrogen-bonding interactions between the bases in GUA5 and CYT16 because of the loss of the guanine N1 H upon covalent attack by mitomycin C and the consequent pulling of GUA5 into the major groove (see Figure 5a). The pairing energy between these two bases is higher than in the other GC pairs by about 12–13 kcal/mol. The rest of the base pairs in this complex are generally unaltered. The effect of covalent complexation in M_{a1} is also seen on some of the base-stacking interactions. Partial loss of stacking between CYT4 and GUA5 and CYT6 and GUA5 contributes to helix destablization in this complex. Typically, the energy loss for each pair is around 2–3 kcal/mol. On the other hand, in the minor-groove complex, the disruption in hydrogen-bonding interactions between the bases in CYT16 and GUA5 is comparatively much smaller as the guanine covalently bound to the drug is not pulled into the minor groove. The pairing energy between these two bases is higher than in other GC base pairs only by about 1.5 kcal/mol. Further, the stacking interactions betwen the base in GUA5 and the neighboring cytosines are not much altered.

(3) Covalently Cross-Linked Complexes between MC and GC10. In these complexes, both C1 and C10 atoms of MC are involved in covalent linkages with O6 and N2 atoms of two suitable guanine bases. Two possibilities have been examined for the major-groove binding of the drug. In the first one, C1 and C10 atoms have been covalently bonded to O6 of GUA5 and GUA15, respectively, while in the other, they are bonded, respectively, to O6 of GUA15 and GUA5. These two covalent complexes have been referred to as C_1 and C_2, respectively. Only one possibility was considered for minor-groove binding of the drug. Here, the C1 and C10 atoms of MC were covalently bonded to N2 of GUA5 and GUA17, respectively. This complex has been referred to as C_3. Initial model building revealed that the other model in which the C1 and C10 atoms of the drug are covalently bonded to N2 of GUA17 and GUA5, respectively, had several short contacts between the polynucleotide and the drug and thus was unlikely to be as stable as C_3. Hence, this model was not considered for energy refinement. It may be pointed out that crystallographic analyses[31-33] of a few derivatives of mitomycin reveal the distance between C1 and C10 to be very similar to that between O6 atoms of guanines, which are located on either strand of a DNA duplex and are involved in neighboring base pairs. This is also true of N2 atoms of guanines.

Drug in the Major Groove. Parts a and b of Figure 7 show stereopairs of the two structures C_1 and C_2, respectively. As in

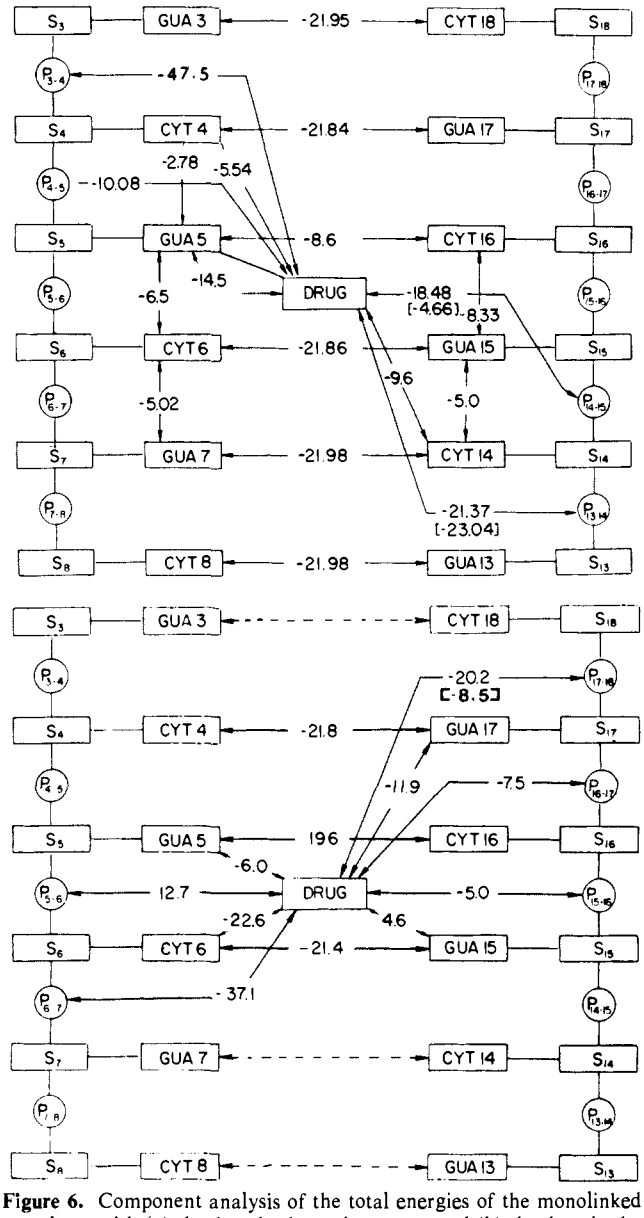

Figure 6. Component analysis of the total energies of the monolinked complexes with (a) the drug in the major groove and (b) the drug in the minor groove. Here, the sugars and bases are represented by rectangular boxes (marked S and the base name as in text, respectively). The phosphate groups are represented by circles (marked P_{n-m} as defined in text). The interactions and their energies between various groups are represented by arrows connecting the appropriate boxes. The energy values without parentheses or square brackets correspond to M_{a1} in (a) and M_{a2} in (b) and those in square brackets to MA_{m1} in (a) and MA_{m2} in (b). Only when interactions are signficantly different (by at least 2 kcal/mol) in these complexes are they indicated in the diagrams. Thus, only a single energy value connecting two groups in (a) or (b) means that the corresponding value in the other structure is very similar.

the case of the monolinked complexes, the sugars in CYT2 and CYT12 of both the cross-linked complexes are puckered with O1′ endo–C1′ exo geometries (W = 111°). The sugars in GUA3 and GUA13 have C1′ exo puckers in C_2 (W = 137° and 140°, respectively), and that in GUA15 has a C3′ endo pucker (W = 12°). On the other hand, in C_1 the pucker of the sugar corresponding to GUA13 is alone changed to C1′ exo (W = 138°). The phosphodiester conformations in C1 and C_2 differ significantly, unlike in the case of the monolinked complexes. For example, the P–O_3′ torsion corresponding to P_{3-4}, P_{5-6}, and P_{6-7} differs in the two structures by large amounts (between 30° and 60°). In contrast to these variations on strand 1, on strand 2 only the ω's corresponding to P_{15-16} differ from the others by a significant amount of 63°. The glycosidic orientations of all the bases are anti, but the range of χ in C_1 and C_2 is much larger than that

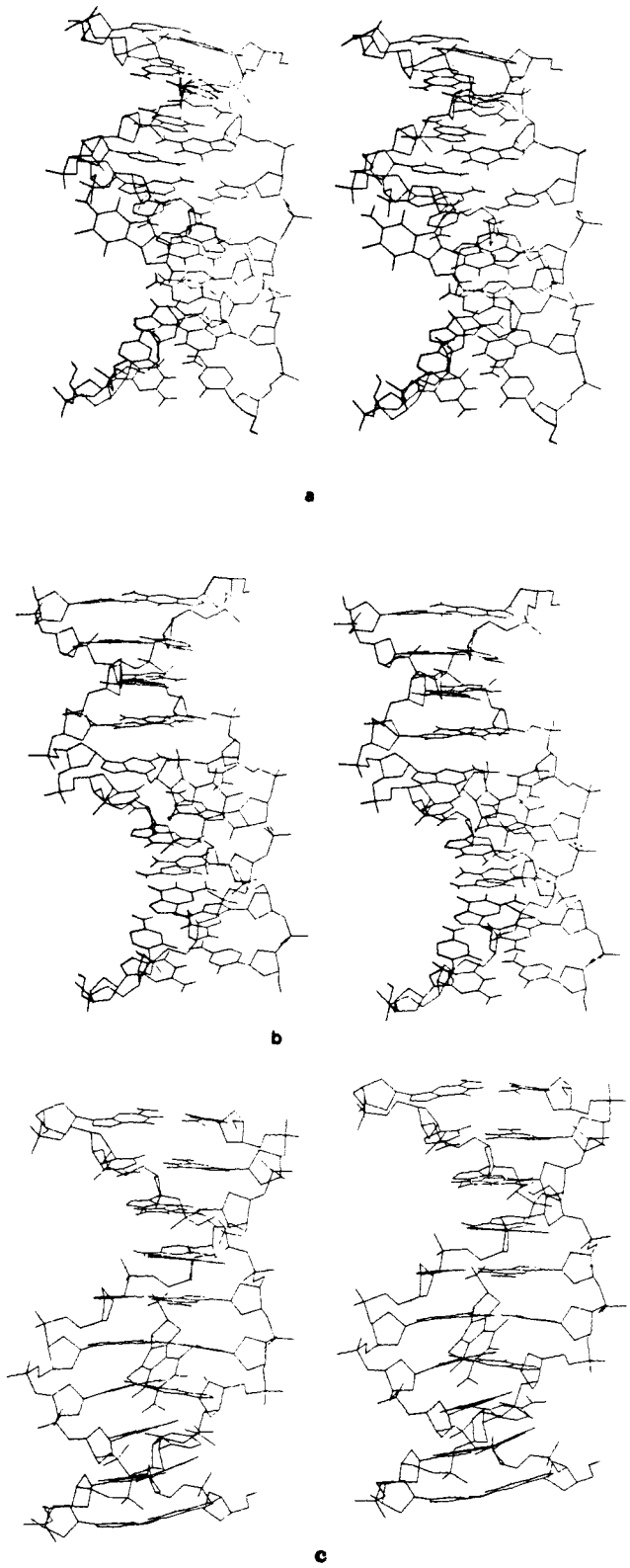

Figure 7. Stereopairs of cross linked covalent complexes between MC and GC10 with (a) the drug in the major groove with C1 and C10 of MC bonded to O6 of GUA5 and GUA15, respectively; (b) the drug in the major groove with C10 and C1 of MC bonded to O6 of GUA5 and GUA15, respectively; and (c) the drug in the major groove with C1 and C10 of MC bonded to N2 of GUA5 and GUA15, respectively.

in the case of the corresponding major-groove monolinked complexes, ranging from 32 to 91°.

In C_1, the two N--H···O hydrogen bonds have acceptor atoms as one of the pendant oxygens in P_{14-15} and P_{3-4}, with the donors being one of the hydrogens in the amino groups at C7 and C2 in MC, respectively. In C2, however, one of the two N--H···O

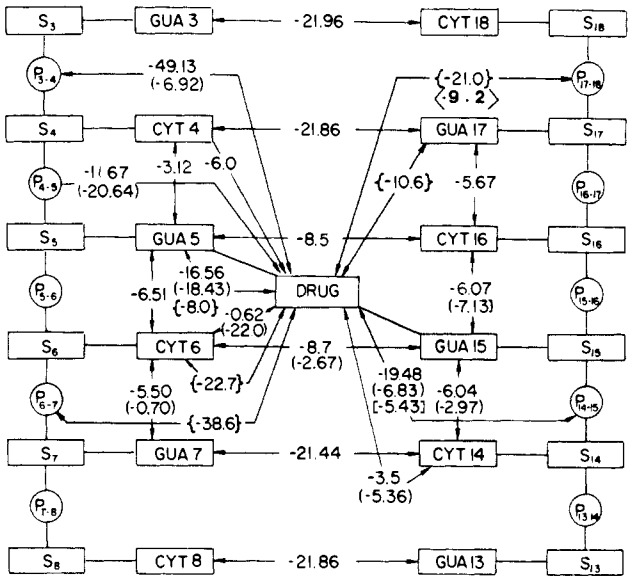

Figure 8. Component analysis diagram corresponding to the cross-linked complexes C_1, C_2, C_3, MA_{c1}, and MA_{c2}. The interaction energies corresponding to these three structures are represented, respectively, without brackets, within parantheses (), within braces {}, within square brackets [], and within Dirac brackets ⟨⟩. Here, the energy values are indicated only if they differ in these structures by more than 2 kcal/mol.

hydrogen bonds has one f the pendant oxygens on P_{4-5} as an acceptor atom with a hydrogen in C7 amino group in MC as a donor. The other bond involves O6 of GUA7 and N2 of MC.

Drug in the Minor Groove. Figure 7c shows a stereopair of the cross-linked complex C_3. For reasons stated earlier, we did not carry out energy refinement of a cross-linked complex in which the drug is in the minor groove and the cross-linking arrangement corresponds to that in C_2. The sugars in CYT2, GUA3, CYT4, CYT12, GUA13, and CYT18 have geometries in the C1′ exo region with W values of 128°, 125°, 102°, 141°, 142°, and 130°, respectively. The P–O3′ bond conformation is trans at the 3′ ends of CYT6, CYT8, GUA15, CYT16, and CYT18. This complex is stabilized by two hydrogen bonds (both N--H···O) between the polynucleotide and the drug (Table I). The acceptor atoms in the two hydrogen bonds are O_2 in CYT6 and one of the pendant oxygens in P_{17-18}. The corresponding donor atoms in the drug are one of the hydrogens in the amino group at C7 and C2, respectively.

Energetics of Cross-Linked Complexes. Despite the conformational variations between the two cross-linked structures C_1 and C_2, their total energies differ by less than 1 kcal/mol. However, the drug–helix and helix destabilization energies differ in the two structures (Table II). Cross-linking affects the base pairs GUA15–CYT6 and GUA5–CYT16 and the interactions between them. The salient features of various interactions in the two complexes are highlighted in the component analysis diagrams presented in Figure 8, which reveals the following points of interest. As stated earlier, C_1 is stabilized by favorable hydrogen-bonding and electrostatic interactions between the protonated amino group at C2 in MC and P_{3-4} and between the amino group at C7 in MC and P_{14-15}. It may be noted that these two sets of interactions are absent in C_2, which is stabilized by hydrogen-bonding interactions between P_{4-5} and the amino group at C7 in mitomycin C. The latter feature was absent in the monolinked complexes. The stabilization of C_3 by hydrogen-bonding interactions with P_{17-18} and CYT6 is also evident in the component analysis diagram (Figure 8). In addition, this complex is also stabilized by favorable electrostatic interactions with P_{6-7}, as was the case in the monolinked complex M_{a2}.

One of the main distinguishing features between the two structures is the position of the protonated amino group. In C_1, it is similar to that in M_{a1}, whereas in C_2 it is quite different. In the latter, this group juts in between the two base pairs CYT6–GUA15 and GUA7–CYT14, resulting in hydrogen-bonding interactions between O6 of GUA7 and N2 of MC (Figure 7b). Figure 7a clearly demonstrates the absence of such interactions in C_1. Figure 7b shows that this hydrogen-bond formation causes disruption of hydrogen-bonding interactions between the bases in GUA15 and CYT6 as is reflected in the total interaction energy of −2.7 kcal/mol (as against −20 to −21 kcal/mol in the case of the other G–C base pairs). This also causes the cytosine in CYT6 to move away from the helix axis and be almost on top of the C2′, C1′, and N9 atoms of GUA5. This change is reflected in the glycosidic torsion in that residue going to a value of 91°. It is of interest to note that only the base pairs involving GUA5 and those 3′ to it are disrupted to varying extents due to the formation of this complex. On the other hand, the pairs involving bases at the 5′ end of GUA5 have almost the standard Watson–Crick base-pairing configuration. This situation is in contrast to that of C_1 where only the bases involved in cross-linking are swung into the major groove, whereas the rest of them remain essentially unaltered.

(4) Monolinked and Cross-Linked Complexes between GC10 and MA. In these two complexes also, only the possibility of axial orientation of the protonated amino group has been examined. These complexes have been referred to as MA_{m1} and MA_{c1} when the drug is in the major groove and as MA_{m2} and MA_{c2} when the drug is in the minor groove.

DNA–Mitomycin A Monolinked Complexes. For the reasons stated above, we have built the mitomycin A–GC10 complex with the axial orientation of the protonated amino group in the drug. MA differs from MC in the substitution at C7, which is an O-methyl group in the former and an amino group in the latter. The configuration of this *O*-methyl group used in the present study is the same as has been observed in a few crystal structures of MA derivatives.[31,32] The conformational features of the polynucleotide backbone and the base orientations in MA_{m1} and MA_{m2} are very similar to those of the corresponding monolinked complexes involving MC. The only significant difference in the two sets of complexes is the hydrogen-bonding interaction profile. It is obvious that the substitution of the NH_2 group at C7 by an *O*-methyl group deprives the DNA–MA complex of one of the N--H···O hydrogen bonds that was formed between the above said NH_2 and one of the phosphate groups in the polynucleotides in both M_{a1} and M_{a2} (Table I).

The total energy of MA_{m1} is higher than that of M_{a1} by 8 kcal/mol. This difference is manifested almost entirely in the drug–helix interaction energy (see Table II). This is not surprising in view of the loss of a hydrogen bond in the monolinked complex involving MA compared to MC. The energy component analysis of MA_{m1} (Figure 6a) reveals that, as in M_{a1}, the base in GUA5 gets pulled out into the major groove. As is to be expected, the helix destabilization energy of MA_{m1} is almost the same as that of M_{a1}.

The total energy of MA_{m2} is also higher than that of M_{a2} by about 6 kcal/mol. The helix destabilization energies of these two structures are almost the same. Here, too, the difference in total energies is mainly due to reduced interaction energy between the drug and the polynucleotide in MA_{m2} compared to M_{a2}. unlike the case of MA_{m1}, in MA_{m2} the base pair GUA5–CYT16 is not disrupted.

DNA–Mitomycin A Cross-Linked Complexes. It is likely that our calculations, which do not explicitly include counterion–solvation effects, would overestimate the stabilization due to the stronger electrostatic interactions between the drug and the polynucleotide in C_2. Thus, we consider C_1 to be the more reasonable structure and have restricted our calculations on the cross-linked complexes between mitomycin A and GC10 to that of the C_1 type. As is to be expected from the study of the corresponding monolinked complexes, here too the only difference between MA_{c1} and C_1 is the hydrogen bond involving the phosphate group intervening CYT14 and GUA15. In the former it is absent because of the *O*-methyl substitution at C7 rather than an amino group in the latter. This situation is also true when the drug is in the minor groove.

Table III. Quantum Chemical Charges on Mitomycin A and Mitomycin C in Complexes with GC10

I[a]		II[b]		III[c]		IV[d]		V[e]	
C1	0.3350	C1	0.4020	C1	0.4020	C1	0.4020	C1	0.4020
C2	0.3350	C2	0.2590	C2	0.2590	C2	0.2590	C2	0.2590
N2	-0.3810	N2	-0.2820	N2	-0.2820	N2	-0.2820	N2	-0.2820
HN2A	0.3560	HN2A	0.3060	HN2A	0.3060	HN2A	0.3060	HN2A	0.3060
HN2B	0.3560	HN2B	0.3060	HN2B	0.3060	HN2B	0.3060	HN2B	0.3060
		HN2B	0.3060	HN2B	0.3060	HN2B	0.3060	HN2B	0.3060
C3	0.2220	C3	0.1870	C3	0.1870	C3	0.1870	C3	0.1870
N4	0.0510	N4	0.0510	N4	0.0510	N4	0.0510	N4	0.0510
C4A	-0.1200	C4A	-0.1200	C4A	-0.1200	C4A	-0.1200	C4A	-0.1200
C5	0.4670	C5	0.4670	C5	0.4670	C5	0.4670	C5	0.4670
O5	-0.3480	O5	-0.3480	O5	-0.3480	O5	-0.3480	O5	-0.3480
C6	-0.2330	C6	-0.2330	C6	-0.2330	C6	-0.2330	C6	-0.2330
C6M	0.0540	C6M	0.0540	C6M	0.0540	C6M	0.0540	C6M	0.0540
C7	0.0920	C7	0.0920	C7	0.0920	C7	0.1200	C7	0.1200
N7	-0.5130	N7	-0.5130	N7	-0.5130	O7	-0.2730	O7	-0.2730
HN7A	0.2700	HN7A	0.2700	HN7A	0.2700	C7M	0.2720	C7M	0.2720
HN7B	0.2700	HN7B	0.2700	HN7B	0.2700	C8	0.4700	C8	0.4700
C6	0.4700	C8	0.4700	C8	0.4700	O8	-0.2970	O8	-0.2970
O8	-0.2970	O8	-0.2970	O8	-0.2970	C8A	-0.2160	C8A	-0.2160
C8A	-0.2160	C8A	-0.2160	C8A	-0.2160	C9A	-0.2610	C9A	-0.2610
C9A	-0.2210	C9A	-0.2610	C9A	-0.2610	C9	0.0500	C9	0.0500
C9	0.0500	C9	0.0500	C9	0.0500	C10	0.2360	C10	0.2220
C10	0.2360	C10	0.2360	C10	0.2220	O10	-0.4590		
O10	-0.4590	O10	-0.4590			C10A	0.9480		
C10A	0.9480	C10A	0.9480			O10A	-0.5300		
O10A	-0.5300	O10A	-0.5300			N10A	-0.9060		
N10A	-0.9060	N10A	-0.9060			HN41	0.3560		
HN41	0.3560	HN41	0.3560			HN42	0.3560		
HN42	0.3560	HN42	0.3560						

[a] Mitomycin C involved in noncovalent complexes. [b] Mitomycin C involved in monolinked complexes. [c] Mitomycin C involved in cross-linked complexes. [d] Mitomycin A involved in monolinked complexes. [e] Mitomycin A involved in cross-linked complexes

The absence of this hydrogen bond leads to a reduction in the drug–helix interaction energies of the complexes MA_{c1} and $MA_{c2'}$ as is evident from Table II. The helix destabilization energies are nearly the same as those of the corresponding complexes with mitomycin C. The component analysis diagram presented in Figure 8 reveals that, as in C_1, only the base pairs that are directly involved in the covalent linkages are disrupted, and this is manifested by significantly reduced base pair energy. The rest of the base pairs are unaltered.

Discussion and Conclusions

A number of models for the complex between B DNA and mitomycin have been investigated. The most striking of the aspects of conformational features in all the complexes, both noncovalent and covalent, is the stabilization achieved through an extended network of hydrogen bonds between the polynucleotide and the drug. The orientations of the drug in the major and the minor grooves in most of the complexes are such as to promote these interactions for most of the proton donating and accepting groups on the drug. However, the B DNA configuration in all the complexes is not significantly altered. Conformational disturbances, small in magnitude, are confined to a stretch of two to three base pairs around the site of complexation. This implies that mitomycin–DNA complexes can be formed without distorting the latter drastically, unlike what occurs upon alkylation by nitrogen mustard gas.[11,24]

What do our models suggest about the mechanism of covalent complex formation between mitomycin and DNA? The nonintercalation complexes are energetically favored over the intercalation complexes, irrespective of whether the drug is in the major or minor groove. Further, as stated earlier in this paper, the energetically most favorable intercalation models we could build were characterized by trans,trans phosphodiester conformations at the intercalation site, which have not been observed in the crystallographic analyses of complexes between intercalating drugs and nucleic acid fragments.[53-55] Therefore, our calculations suggest that mitomycins are less likely to intercalate in an initial noncovalent environment, though some experimental studies have suggested such a model as a plausible one.[34] Also, in an intercalated complex, the drug will not be suitably oriented to promote covalent interactions between C1 on the drug and O6 (or N2) on guanine with the right configuration.

The noncovalent, nonintercalation complex with the drug in the major groove is energetically favored over the corresponding minor-groove complex. This is because of the fewer hydrogen-bonding interactions between the drug and the polynucleotide in the latter, which is also reflected in the higher drug–helix interaction energies. If this initial calculated noncovalent binding energy reflects the probability of major-vs. minor-groove attack and the subsequent chemical reactions are facile for either groove, one can understand why the major-groove attack is more probable than the minor-groove attack, as observed. The conformational features of these complexes seem to suggest that the drug is initially directed into the appropriate conformational environment by the favorable secondary interactions with the polynucleotide. In this environment, covalent binding can take place either between C1 (MC) and O6 or C1 and N7 in the major groove and between C1 and N2 in the minor groove.

The major-groove covalent (monolinked) complexes (involving O6 of guanines) are energetically destablized relative to their minor-groove counterparts (involving N2 of guanines). This is not surprising because of the fact that, in the former, the covalently attached guanine loses its N1 proton and to retain optimum hydrogen bonding with the cytosine in the opposite strand is "pulled" out into the major groove, thus reducing stacking interactions. However, in the latter complex, such a disruption of the base pairs is absent as the Watson–Crick hydrogen bonding and stacking of the covalently attached base is not much altered. In the case of the cross-liked complexes, this relative destablization is further magnified as a result of two base pairs being disrupted in the major-groove cross-linking reaction, whereas the base pairs

(53) Reddy, B. S.; Seshadri, T. P.; Sakore, T. D.; Sobell, H. M. *J. Mol. Biol.* **1979**, *135*, 787–812.

(54) Wang, A. H.-J.; Nathans, J.; van der Marel, G.; van Boom, J. H.; Rich, A. *Nature (London)* **1978**, *276*, 471–474.

(55) Shieh, H. S.; Berman, H. M.; Dabrow, M.; Neidle, S. *Nucleic Acids Res.* **1980**, *8*, 85–97.

Table IV. Data for Appendix II

bond	K_r	r_{eq}	bond	K_r	r_{eq}
CH-CZ	260	1.510	cQ-C3	260	1.505
CZ-CZ	470	1.378	CQ-N	475	1.341
CZ-C2	260	1.501	CQ-CQ	470	1.347
OZ-C2	260	1.510	CQ-CY	360	1.485
CH-N3	250	1.542	CQ-CZ	410	1.439
C2-N*	340	1.458	CY-N	457	1.310
CZ-N*	425	1.381	CY-OY	570	1.224
CQ-N*	425	1.376	OZ-CY	320	1.390

angle	K_ϑ	ϑ_{eq}	angle	K_ϑ	ϑ_{eq}
C2-CH-NW	50	118.4	OZ-CY-N	80	110.6
CH-CH-NW	100	60.2	C2-OZ-CY	63	114.6
CH-NW-CH	100	59.7	CZ-C2-OZ	63	104.7
H3-NW-H3	50	117.0	CZ-N*-CQ	80	107.8
H3-NW-CH	50	117.0	C2-N*-CQ	80	136.5
CY-CQ-N	60	115.8	CQ-OS-C3	40	119.0
CH-CZ-CZ	80	142.8	CQ-CQ-OS	80	123.2
CH-CZ-N*	80	107.0	CY-CQ-OS	80	115.8
CZ-CZ-N*	80	110.2	N*-C2-CH	60	101.5
CZ-CZ-C2	80	126.5	N3-CH-C2	60	112.0
CZ-CZ-CQ	80	104.1	N3-CH-CH	60	112.0
CZ-CQ-CQ	80	111.2	H3-N3-CH	40	110.4
N*-CQ-CQ	80	107.2	CZ-N*-C2	65	115.7
N*-CQ-CY	80	131.8	CZ-CH-CH	35	103.5
C3-CQ-CY	75	118.3	C2-CZ-CQ	65	129.4
C3-CQ-CQ	75	120.7	OY-CY-N	65	129.7
CQ-CQ-N	80	123.2	OS-CH-CZ	40	112.0
CY-CQ-N	80	115.8	CQ-N-H	40	120.6
CQ-CQ-CY	80	121.0	NH-CH-CZ	50	112.0
CQ-CY-CQ	80	116.0	NB-CH-CH	50	112.0
CQ-CY-OY	80	121.0	N2-CH-CZ	40	112.0
CZ-CQ-CY	80	127.8	N2-C2-CZ	40	112.0
OZ-CY-OY	80	119.7	OS-C2-CZ	40	112.0

dihedral angle	m^a	V_n	γ	n	dihedral angle	m^a	V_n	γ	n
X-CZ-CH-X	4	0.3	180	3	X-CQ-N*-X	4	6.4	180	2
X-OS-CQ-X	2	1.5	180	3	X-CZ-N*-X	4	6.0	180	2
X-NW-CH-X	1	0.0	0	3	X-CZ-C2-X	2	0.3	180	3
X-CZ-CZ-X	4	13.2	180	2	X-OZ-C2-X	1	0.5	0	3
X-CZ-CQ-X	4	3.4	180	2	X-OZ-CY-X	2	4.0	180	2
X-CQ-CQ-X	4	25.6	180	2	X-N-CY-X	4	18.1	180	2
X-CQ-CY-X	4	5.0	180	2	X-N3-CH-X	6	0.0	180	2
X-CQ-N-X	4	9.5	189	2	X-N*-C2-X	2	6.0	180	2

[a] m = multiplicity of the dihedral angle.

are intact in the minor-groove cross-linking reaction.

The molecular mechanical calculations are unable to exclude monolinked complex formation between mitomycin on one hand and (a) poly(dG)·poly(dC) with O6 alkylation and (b) poly(dG-dC)·poly(dG-dC) with N7 alkylation. In both the complexes, however, cross-linking is not possible. In the former the cytosines on the opposite strand do not offer any potential binding sites for the drug, while in the latter, the distance between N7 atoms on the guanines of the opposite strand, involved in neighboring base pairs, is too large (~7 Å) for the cross-linking to be achieved.

Our studies also indicate that the drug–helix interaction energy is more favorable in the case of mitomycin C than in mitomycin A. However, the complexes with these drugs have very similar polynucleotide destabilization energies. Though our calculations predict stronger binding to DNA by MC than by MA, the differences in the binding energies for these two drugs cannot be directly correlated to the experimentally observed biological activities.

The conformational features of our models suggest that the guanine bases involved in covalent linkages with the drug could be locked in the anti orientations associated with the B form and thus could be prevented from undergoing a rotation to the *syn* conformation associated with the Z form. This could lead to blocking of the B–Z transition that has been recently implicated in the transcriptional activity of the genes.[56] Such locking of bases could also play a significant role in preventing transitions to any other polymorphic form of significance in DNA replication and transcription. These facts are consistent with some of the experimental studies on other cross-linking agents that have been shown to block B–Z transitions in native and synthetic polynucleotides.[57-59]

We emphasize that the molecular mechanical approach employed here is not capable of giving a quantitative analysis of the free energies of mitomycin–DNA interactions or of the energetics for the reaction pathway of the covalent attack. One of the reviewers has pointed out (and we agree) that we have not made an exhaustive study of all possible intercalation models in order to "add confidence to the significance of the findings". We emphasize that even if a detailed search was made, a more quantitative comparison of those structures would not be meaningful due to the inherent inaccuracies of the relative energies coming from the lack of explicit solvation and counterion atmosphere in the calculations. The main goal of our present investigations has been to obtain useful qualitative insight into these complexes, which would provide further impetus for 2D NMR/NOE and crystallographic studies on oligonucleotide complexes with the mitomycins.

(56) Razin, A.; Riggs, A. D. *Science (Washington, D.C.)* **1980**, *210*, 604–610.

(57) Malfoy, B.; Hartmann, B.; Leng, M. *Nucleic Acids Res.* **1981**, *9*, 5659–5669.

(58) Ushay, H. M.; Santella, R. M.; Caradonna, J. P.; Grunberger, D.; Lippard, S. J. *Nucleic Acids Res.* **1982**, *10*, 3573–3587.

(59) Floro, N. A.; Wetterhahn, K. E. *Biochem. Biophys. Res. Commun.* **1984**, *124*, 106–113.

Acknowledgment. We thank Professor W. A. Remers for suggestions and useful discussions. We gratefully acknowledge the support of the National Cancer Institute (Grant CA-25644) in this research. The use of the facilities of the UCSF Computer Graphics Laboratory (R. Langridge, Director, and T. Ferrin, Facility Manager), supported by NIH Grant RR-1081, is also gratefully acknowledged.

Appendix I

The chemical charges on mitomycin A and mitomycin C in the monovalent and covalent complexes with the decamer GC10 are listed in Table III.

Appendix II

The bond length, bond angle, and dihedral angle parameters corresponding to the additional atomic species types defined for mitomycin A and mitomycin C in their covalent and noncovalent complexes with the polynucleotide GC10, investigated in this study are listed in Table IV.

The species types used for the atoms of mitomycin are indicated within parentheses along with the names of the atoms as follows: C1 (CH), C2 (CH), N2 (N3), C3 (C2), N4 (N*), C4A (CQ), C5 (CY), O5 (OY), C6 (CQ), CM6 (C3), C7 (CQ), N7 (N), C8 (CY), O8 (OY), C8A (CQ), C9 (CZ), C9A (CZ), C10 (C2), O10 (OZ), C10A (CY), O10A (OY), N10A (N). The hydrogens in the amino groups at the C7 and C10A atoms were assigned the species type H, and those at C2 were assigned H3. In the case of the noncovalent complexes, N2 was assigned NW and the corresponding hydrogen HW. The parameters corresponding to HW are the same as those of H3. In the case of mitomycin A, the oxygen and the methyl atoms at C7 were respectively assigned OS and C3 species types.

Combined Chemical and Enzymatic Synthesis of Sialyloligosaccharides and Characterization by 500-MHz ^{1}H and ^{13}C NMR Spectroscopy

Subramaniam Sabesan† and James C. Paulson*

Contribution from the Department of Biological Chemistry, UCLA School of Medicine, Los Angeles, California 90024. *Received August 22, 1985*

Abstract: Sialyloligosaccharides that occur as terminal sequences in glycoproteins and glycolipids were synthesized by using combined chemical and enzymatic methodologies. Neutral oligosaccharides containing βDGal(1,3)βDGlcNAc (type 1), βDGal(1,4)βDGlc(NAc) (type 2), and βDGal(1,3)βDGalNAc (type 3) sequences were sialylated enzymatically by using three purified mammalian sialyltransferases each of which uses one of these above three sequences as a substrate. In each case a single oligosaccharide was produced that could be quantitatively purified by simple isolation procedures. In all, ten sialyloligosaccharides, including six which are novel, were prepared in 10–20-μmol scale. In addition, three more sialyloligosaccharides were isolated from a mixture of human or bovine milk oligosaccharides. All these compounds have been characterized by 500-MHz ^{1}H and ^{13}C NMR spectroscopy with complete assignments of ^{13}C chemical shifts. A comparison of the proton and ^{13}C chemical shifts in these linear sialosides with those published for branched structures found in gangliosides GM_1 and GM_2 indicates significant differences, especially for the atoms around the sialoside linkages, and a rationale for these differences based on the steric environment around these atoms in the linear sialosides and branched structures is discussed.

Sialyloligosaccharides of glycoproteins and glycolipids are known to mediate a variety of biological processes.[1] For example, sialyloligosaccharides serve as cell surface receptor determinants for influenza virus and other viruses,[2] for mycoplasma,[3,4] for blood group and tumor specific antibodies,[1,5] for interferon,[6] for recirculating lymphocytes seeking capillary sites of entry to the lymph system,[7] for bacterial toxins,[1] and for a variety of plant and animal lectins.[8,9] The diversity of sialyloligosaccharide sequences which occur naturally are evident in the most common carbohydrate groups of glycoproteins and glycolipids.[10,11] Thus, sialic acid[12] is frequently attached in 2,3 or 2,6-linkage to galactose, *N*-acetylglucosamine, or *N*-acetylgalactosamine and in the 2,8 linkage to another sialic acid in the terminal sequences (I–V) of glycoprotein oligosaccharides N-linked to asparagine or O-linked to threonine or serine.[13] Similar sequences and additional variation in structures are seen in the carbohydrate groups of glycolipids[14] as illustrated by ganglioside GT_{1b} (VI). Such diversity in structure

αDNeuAc(2,6)βDGal(1,4)βDGlcNAc-R (I)

αDNeuAc(2,3)βDGal(1,4/3)βDGlcNAc-R (II)

αDNeuAc(2,3)βDGal(1,3)
βDGlcNAc-R (III)
αDNeuAc(2,6)

αDNeuAc(2,8)αDNeuAc(2,3)βDGal-R (IV)

αDNeuAc(2,3)βDGal(1,3)
αDGalNAc-*O*-Thr/Ser (V)
αDNeuAc(2,6)

† Present address: E. I. Dupont de Nemours & Co. Inc., Chemical Sciences Division, Experimental Research Station, Wilmington, DE 19898.

(1) Schauer, R. *Adv. Carbohydr. Chem. Biochem.* **1982**, *40*, 131.
(2) Paulson, J. C. In "The Receptors"; Conn, M., Ed.; Academic Press: New York, 1985; Vol. 2, p 131.
(3) Glasgow, L. R.; Hill, R. L. *Infect. Immun.* **1980**, *30*, 353.
(4) Loomes, L. M.; Uemura, K.; Childs, R. A.; Paulson, J. C.; Rogers, G. N.; Scudder, P. R.; Michalski, J.; Hounsell, E. F.; Taylor-Robinson, D.; Feizi, T. *Nature (London)* **1984**, *307*, 560.
(5) Hakomori, S. *Annu. Rev. Immunol.* **1984**, *2*, 103.
(6) Ankel, H.; Krishnamurti, C.; Besancon, F.; Stefanos, S.; Falcoff, E. *Proc. Natl. Acad. Sci. U.S.A.* **1980**, *77*, 2528.
(7) Rosen, S. D.; Singer, M. S.; Yednock, T. A.; Stoolman, L. M. *Science* (Washington, D.C.) **1985**, *228*, 1005.
(8) Pardoe, G. I.; Uhlenbruck, G. *J. Med. Lab. Technol.* **1970**, *27*, 249.
(9) Ravindranath, M. H.; Higa, H. H.; Cooper, E. L.; Paulson, J. C. *J. Biol. Chem.* **1985**, *260*, 8850.
(10) Montreuil, J. *Adv. Carbohydr. Chem. Biochem.* **1980**, *37*, 157.
(11) Kobata, A. In "Biology of Carbohydrates"; Ginsburg, V., Robbins, P. W., Eds.; John Wiley and Sons: New York, 1984; Vol. 2, p 87.
(12) Sialic acid comprises a family of derivatives of neuraminic acid (5-amino-3,5-dideoxy-D-*glycero*-nonulosonic acid. In this text it refers only to the *N*-acetyl neuraminic acid.
(13) In sequences I–IV, the R indicates the remainder of the oligosaccharide, which in the case of *N*-linked oligosaccharides is the $Man_3GlcNAc_2$ core region.
(14) Ledeen, R. W.; Yu, R. K. *Methods Enzymol.* **1982**, *83*, 139.

0002-7863/86/1508-2068$01.50/0